UDC 539.3

ESTABLISHING THE CORRELATION OF THE VERTICAL AND HORIZONTAL PASSIVE FAILURE PRESSURE IN FRONT OF CONSTRUCTED TBM TUNNELS FACE

Nguyen Anh Tuan,
PhD

Tran Van Dung,
M.Eng.

Hochiminh City University of Transport,
No. 2, Vo Oanh St., Ward 25, Binh Thanh Dist., Hochiminh City, Vietnam

DOI: 10.32347/2410-2547.2020.105.34-47

The paper aims to investigate the relationship between factors which have the impacts on the tunnel and the ground and establish formulas to calculate the correlation of the passive failure pressure in front of tunnel face in the vertical and horizontal directions by using the Finite Element Method (FEM).

Keywords: TBM tunnel, FEM, passive failure pressure, tunnel face, sand.

1. Introduction

The Finite Element Method (FEM) was formed from the 40s of the twentieth century and is widely used up to now to find solutions to the problem of elasticity, elasticity - plasticity, ductility - plasticity. Its advantage is taking into account the discontinuity and heterogeneity of stratigraphic structures, which can solve complex boundary problems and calculate the values of stresses - their deformation and distribution. Thanks to these distribution rules, it helps analyze the mechanism of underground construction.

At the beginning of development, numerical analysis was known as a design tool, which was strongly criticized. However, the development of information technology has made a revolution in the field of underground construction. Tunnel construction are calculated with full numerical analysis.

Currently, numerical analysis methods have been simplified and tunnel design is mainly based on experience, intuition and solutions. The underdevelopment of information technology makes the great amount of data be difficult to input and analyze. The difficulty now is solved by powerful computers, user-friendly interface. It also saves time to analyze data from weekly to daily or even hours.

The convenience of numerical analysis methods has been proven. Both the behavior of the materials and boundary conditions have been included in the calculations, and the study of parameters to improve the design of tunnel construction can be done more easily.

2. Literature review

In order to avoid ground loss which can trigger collapse of tunnel face due to instability of surrounding soil, EPB-TBM machine is designed with a closed

boring chamber creating an effective surface stabilization, this makes pressure balance of soils between inside and outside boring machine. Working principle of EPB-TBM is that the excavated soils will be mixed with water, clayey slurry or additives such as foam or polymer. This mixture will form a layer pasting on the boring chamber and creates a balancing pressure versus overburden pressure of ground, and this mixture shall be removed out through conveyors upon completion of construction.

This face pressure shall be kept stably during tunneling process. It is, however that, due to the overburden and water pressures increase from the top to bottom of the tunnel face so the supporting pressure at the bottom must be higher to ensure the balancing condition.

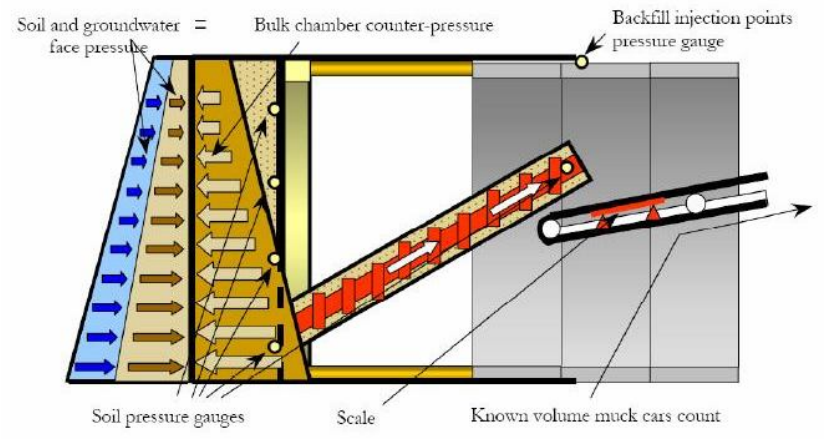

Fig. 1. Schematic representation of the tunnel face pressure control [11]

Broms & Bennermark (1967) evaluated tunnel face stability by using the ratio N which is defined as: [4]

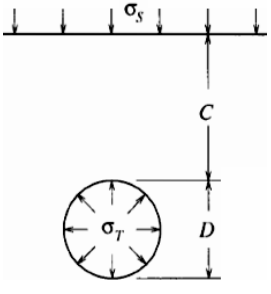

Fig. 2. Cross section of shield tunnelling [7]

$$N = \frac{\sigma_{ob} - \sigma_T}{S_u} = \frac{\sigma_S - \sigma_T + \gamma(C + \frac{D}{2})}{S_u}. \quad (1)$$

Where σ_{ob} is the overburden pressure. And σ_S, σ_T, C, D are defined as Fig. 2.

In the undrained case, all parameters in Equation (1) shall be assumed to be constant, excepting for face pressure σ_T. Hence, N value depends on σ_T. If this supporting pressure reach ultimate value σ_{ob} then tunnel face is completely stable which corresponds to value of $N = 0$.

Davis et. al. (1980) has found four upper bound failure modes which are dependent on tunnel structure as indicated in Fig. 3. [7]

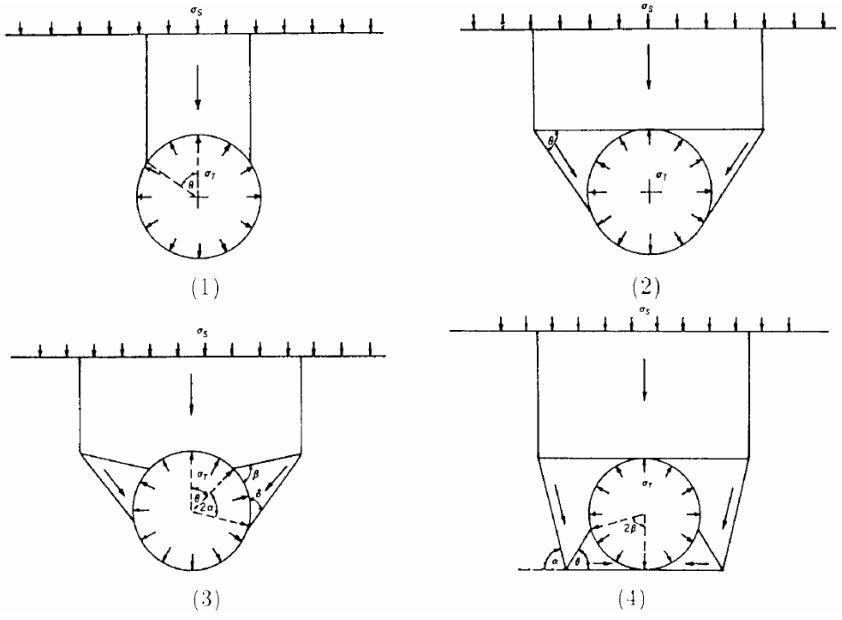

Fig.3. Upper bound failure mechanism [7]

Failure modes (1) and (2) are simple mechanisms, “tunnel roof” and “roof effect and two sides”. Mode (3) is a particular case, covering both (1) and (2). Type (4) is a mechanism with 03 variable angles, saying “tunnel roof side and bottom”.

And lower bound and upper bound stability coefficients with respect to circular tunnel in plane strain condition shall be determined following Fig. 4.

In case of layered soils or soil properties changing over depth, stability coefficient is followed underneath formula:

$$N=\frac{\sigma_S-\sigma_T+\gamma(C+(D/2))}{c_{u0}\left[1+\rho(C+(D/2))\right]}. \quad (2)$$

If assuming stress closed to tunnel crown to be larger than calculated value, then stability coefficient will be:

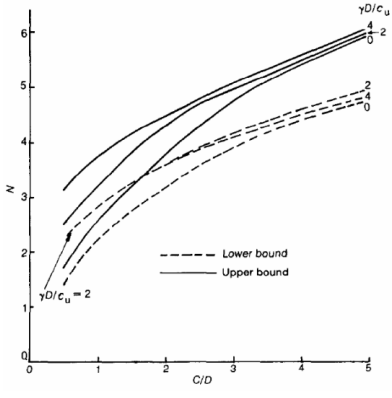

Fig. 4. Upper and lower bound limitation [20]

$$N_{\text{ground}}=\frac{\gamma(C+(D/2))}{c_{u0}\left[1+\rho(C+(D/2))\right]}. \quad (3)$$

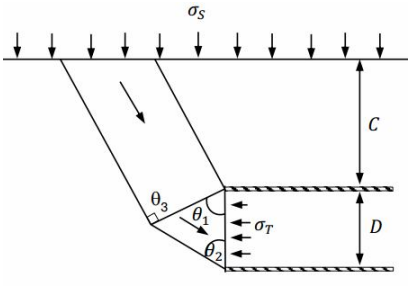

Fig. 5. Upper bound failure mechanism by Davis and partners (1980) [7]

According to Davis et al. (1984), with C/D = 1.5, lower bound and upper bound limits of N vary from 2.9 to 3.4, while $N_{\text{ground}} = 1.67$.

These authors also proposed a upper bound failure mechanism of ground in front of tunnel face based on angles as θ_1, θ_2 and θ_3.

Where:

$$\tan\theta_1 = \tan\theta_2 = 2\sqrt{C/D + 1/4}\,, \quad (4)$$

$$\theta_3 = \pi/2. \quad (5)$$

Table 1

Summary of tunnel face supporting pressure [9]

Tunnel diameter, m	Soil type	Applicable supporting pressure
Earth Pressure Balance (EPB)		
7.45	Soft mud	Earth pressure
8.21	Sand, cohesive soil	Earth pressure + water pressure + 20kPa
5.54	Fine sand	Earth pressure + water pressure + surplus pressure
4.93	Sand, cohesive soil	Earth pressure + 30 to 50 kPa
2.48	Gravel, bed rock, cohesive soil	Earth pressure + water pressure
7.78	Gravel, Cohesive soil, soft soil/mud	Passive earth pressure + water pressure
7.35	Soft soil/mud	Earth pressure +10kPa
5.86	Soft cohesive soil	Earth pressure +20kPa
Slurry Pressure Balance		
6.63	Gravel	Water pressure + 10 to 20kPa
7.04	Cohesive soil	Earth pressure
6.84	Soft cohesive soil, sandy diluvium soil	Passive earth pressure + water pressure +20kPa
7.45	Sandy soil, cohesive soil, gravel	Water pressure +30kPa
10.00	Sandy soil, cohesive soil, gravel	Water pressure +40 to 80kPa
7.45	Sandy soil	Pressure of lost soil + water pressure + surplus pressure
10.58	Sandy soil, cohesive soil	Passive earth pressure + water pressure +20kPa
7.25	Sand, gravel, soft soil	Water pressure + 30kPa

Kanayasu (1995) [9] has summarized many tunneling projects using various methods of creating different supporting pressure of tunnel face. When

EPB shield is used, supporting pressure of tunnel face will depend on geological condition, water pressure and surplus pressure. Mortar EPB shield will be controlled by water pressure to act on active earth pressure and excess pressure. This additional pressure is to prevent unfavorable change of pressure during tunneling works. From Table 1, it can be seen that this additional pressure will be 20 kPa.

Mair (1981) [12] has presented and defined Load Factor (LF) as a ratio of stability coefficient in working condition (service state) over failure state. This factor essentially correlates to stability coefficient against failure:

$$LF = \frac{(\sigma_{V0} - \sigma_i)}{(\sigma_{V0} - \sigma_{ic})}. \quad (6)$$

In which σ_{ic} is value of σ_i at failure moment.

Using this coefficient *LF* is convenient to define safety level of tunnel face [18].

Pavlos Vardoulakis et al. (2009) [24] also implemented scaled-down models to investigate failure mechanism of front soil mass. There were 9 experiments with respect to *C/D* ratios of 0.5; 1 and 2 in dry sand. These experiments models a half of circular-shaped tunnel which is originally 7 m diameter. During experiment process, piston moves backward with constant speed and failure mechanism of ground in front of tunnel face is illustrated in Fig. 6. All failure modes have cylindrical-shaped and runs up to ground surface.

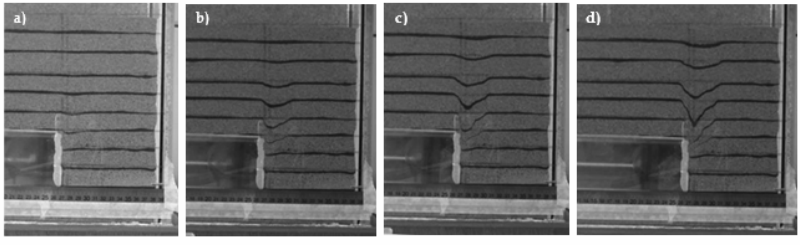

Fig. 6. Test result of *C/D* = 2 [24]

Chambon and Corte (1994) [6] studied failure mechanism and failure active pressure for tunnels embedded at various depth ratio *C/D* ranging from 0.5 - 4.0 by centrifuge tests. Tested dry unit weight of sand was 15.3-16.1 kN/m3, equivalent to void ratios of 0.65-0.92. Prototype diameter of tunnel corresponding to 5m, 10m and 13m were modeled by changing spinning speed of centrifuge machine. Fig. 7. shows the active failure mechanism of tunnels with C/D ratios of 0.5; 1.0 and 2.0. With respect to *C/D* of 0.5, failure mechanism climbs up to ground surface. Fig. 8. shows failure mechanism of 13m-diameter tunnel with *C/D* of 4.0. The observed internal collapse actually caused ground subsidence. It was found that tunnel diameter has a close relationship with failure pressure.

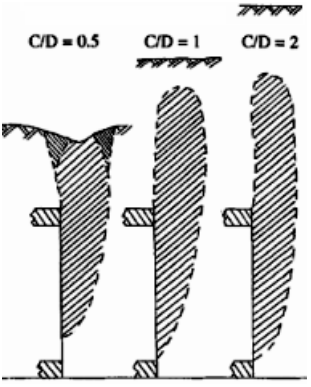

Fig. 7. Failure mechanisms of tunnel *C/D* = 0.5; 1.0 and 2.0 [6]

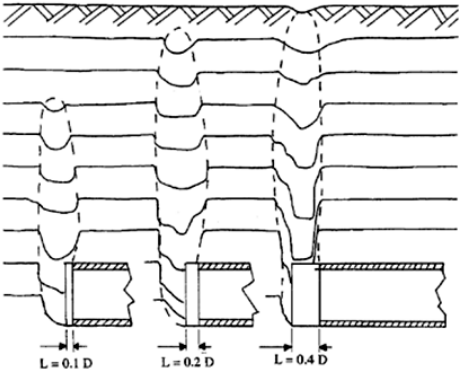

Fig. 8. Failure mechanisms of tunnel face with *D*=13m at *C/D* =4.0, various length of tunnel face [6]

However, surveys on soil around the tunnel are limited. Their disadvantages are not to focus on the soil failure pressure in front of the tunnel face and provide the relationship between factors which have the impacts on the tunnel and the ground. Therefore, the paper helps establish formulas to calculate the correlation of the passive failure pressure in front of tunnel face in the vertical and horizontal directions.

2. Numerical simulation

2.1. Material parameters

Soil parameters for sand and clay and TBM is shown as Table 2.

Table 2

Geological parameters

Soil parameters	Sand	Clay
Saturated unit weight, γ_{sat} (kN/m^3)	20.3	21.1
Unsaturated unit weight, γ_{unsat} (kN/m^3)	19.5	20
Cohesion intercept, c'(kPa)	1.0	300
Angle of friction, φ' (degree)	30^0	1
Angle of dilation, ψ (degree)	0	0
Young modulus, E_{50} (MPa)	27	100
Unloading and reloading modulus, E_{ur} MPa)	81	300
Oedometer modulus, E_{eod} (MPa)	27	100
Poisson's ratio, υ	0.3	0.3
m	0.5	1.0
R_f	0.9	

2.2. Analysis

The tunnel with the 5m diameter is stimulated for cases with *C/D* ratio of 1.5; 2.0; 2.5; 3.3 and 4.0 respectively by using PLAXIS 3D TUNNEL software.

Due to symmetry, only a half of the tunnel was stimulated in this model. The model extended 20m in the z-direction, with the width and depth of 30m and 50.5m respectively. This model is large enough to allow any collapse mechanism to evolve and avoid significantly influence on the boundary of the model.

The interaction between the TBM and soil is defined by the boundary. During excavation, the tunnel pressure is put in the z-direction.

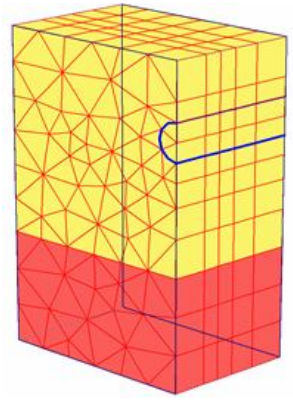

Fig. 9. Finite element mesh adopted for three-dimensional numerical modelling

2.3. Establishing the correlation of passive failure pressure between vertical and horizontal stress in front of the tunnel face

The calculated figures are shown in Table 2.

Table 2

σ_{zz}/σ_{yy} ratio

***C/D*=1.5**		***C/D*=2**		***C/D*=2.5**		***C/D*=3.3**		***C/D*=4**	
σ_{yy}	σ_{zz}	σ_{yy}	σ_{zz}	σ_{yy}	σ_{zz}	σ_{yy}	σ_{zz}	σ_{yy}	σ_{zz}
14.7	11.0	45.5	33.1	51.8	37.1	33.4	22.6	30.7	19.1
71.0	49.0	34.6	22.8	31.4	20.9	66.1	43.7	69.5	41.5
60.2	41.5	92.4	62.2	99.0	67.5	98.3	65.4	117.3	71.0
65.3	44.4	94.8	63.0	120.8	82.5	153.4	102.4	213.6	129.5
153.3	105.6	158.2	107.9	169.2	117.1	208.3	142.3	296.7	175.7
152.6	108.5	185.4	128.3	218.6	150.0	278.1	183.0	338.2	198.6
σ_{zz}/σ_{yy}		σ_{zz}/σ_{yy}		σ_{zz}/σ_{yy}		σ_{zz}/σ_{yy}		σ_{zz}/σ_{yy}	
0.749006		0.728074		0.717220		0.675334		0.622753	
0.690680		0.660592		0.664892		0.661056		0.597708	
0.688416		0.672616		0.681638		0.665371		0.605556	
0.679980		0.664796		0.683047		0.667535		0.606562	
0.689154		0.682144		0.692097		0.683163		0.592043	
0.711103		0.691804		0.686197		0.658096		0.587409	

Let K be a variable depending on the depth of tunnel C and diameter of tunnel D, the relationship of stresses in two directions is shown through K as follows:

$$\sigma_T = K.\sigma_z. \quad (7)$$

To determine the relationship between K and C/D, K_1, K_2, K_3, K_4, K_5 and K_6 is seen as the sections at 8.38406 m, 9.97974 m, 11.38978m 13.64642m, 15.64052 m, 18.83188 m respectively in front of the tunnel face in Z axis.

Based on the data in Table 3, the charts between the parameters are shown in Fig. (10-15).

Table 3

Coefficients K_1, K_2, K_3, K_4, K_5 and K_6

C/D	K_1	K_2	K_3	K_4	K_5	K_6
4	0.622753	0.597708	0.605556	0.606562	0.592043	0.587409
3.3	0.675334	0.661056	0.665371	0.667535	0.683163	0.658096
2.5	0.71722	0.664892	0.681638	0.683047	0.692097	0.686197
2	0.728074	0.660592	0.672616	0.664796	0.682144	0.691804
1.5	0.749006	0.69068	0.688416	0.67998	0.689154	0.711103

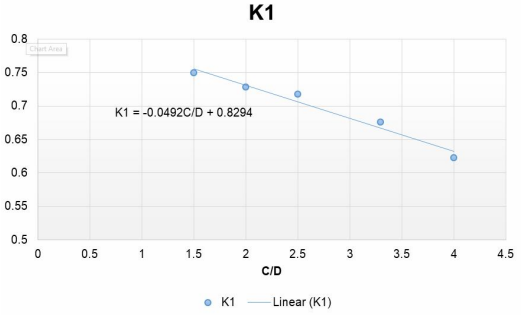

Fig. 10. Relationship chart between K_1 and *C/D*

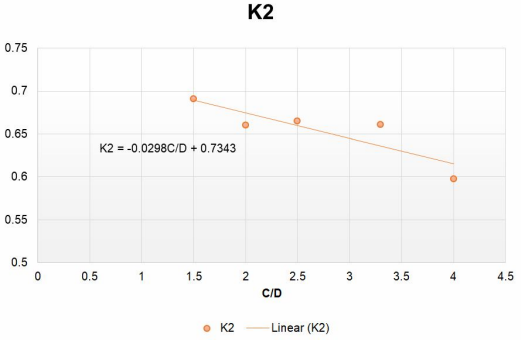

Fig. 11. Relationship chart between K_2 and *C/D*

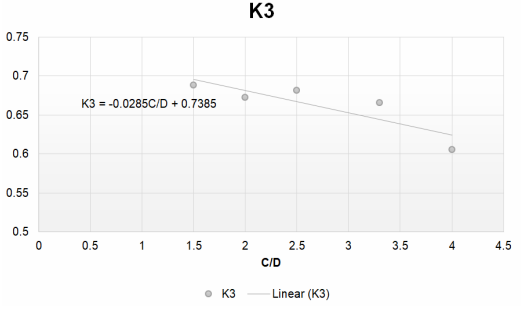

Fig. 12. Relationship chart between K_3 and *C/D*

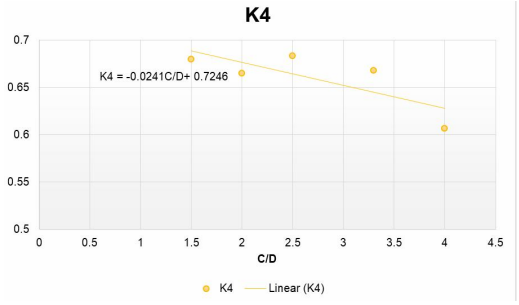

Fig. 13. Relationship chart between K_4 and C/D

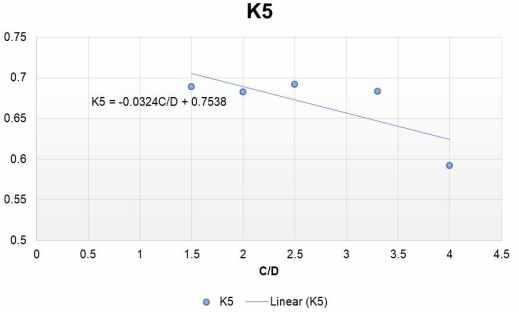

Fig. 14. Relationship chart between K_5 and C/D

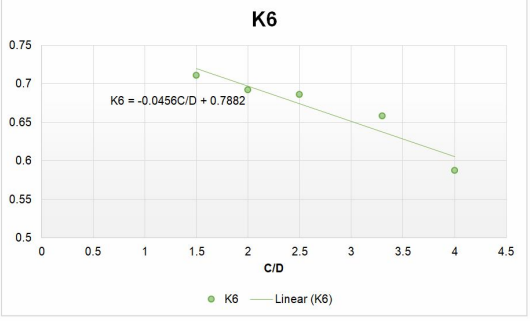

Fig.15. Relationship chart between K_6 and C/D

Let the general formula K be:

$$K = A_1 . \frac{C}{D} + A_2 . \tag{8}$$

K will change with each cross-sectional area in front of the tunnel face with the coefficients A and B in the graphs in Fig. 10 to Fig. 15, we sum them up into Table 4.

Table 4

Coefficients A_1, A_2 and K_1-K_6

Coefficient	A_1	A_2	z, m
K_1	-0.0492	0.8294	8.38406
K_2	-0.0298	0.7343	9.97974
K_3	-0.0285	0.7385	11.38978
K_4	-0.0241	0.7246	13.64642
K_5	-0.0324	0.7538	15.64052
K_6	-0.0456	0.7882	18.83188

Based on the data in Table 4, we use the chart to show the relationship between the coefficient A_1, A_2 and the sections in front of the tunnel face. The charts are shown in Fig. 16 and Fig. 17.

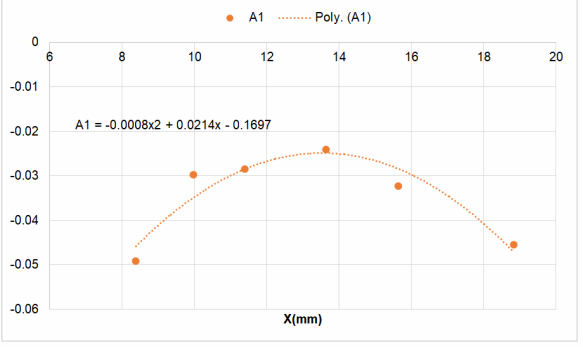

Fig. 16. Chart of A_1 along the vertical axis

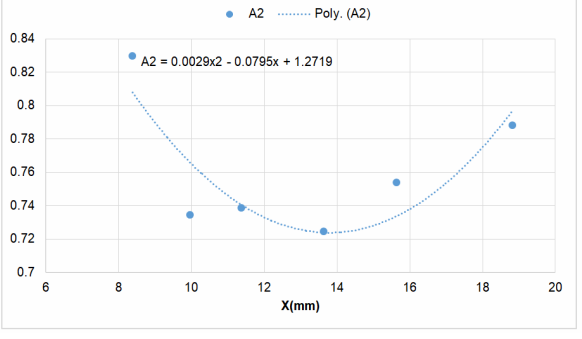

Fig. 17. Chart of A_2 along the vertical axis

The relationship beween K and C/D:

$$K=(-0.0008x^2+0.0214x-0.1697)\frac{C}{D}+0.0029x^2-0.0795x+1.2719. \quad (9)$$

After changing the numbers, we have a table of K coefficient corresponding to the different depths of tunnels as in Table 5.

Table 5

Coefficients $K_{1.5}$, K_2, $K_{2.5}$, $K_{3.3}$ and K_4

Z, m	$K_{1.5}$	K_2	$K_{2.5}$	$K_{3.3}$	K_4
8.38406	0.739443	0.716185	0.692928	0.655716	0.623155
9.97974	0.713622	0.695717	0.677812	0.649165	0.624098
11.38978	0.69801	0.68314	0.66827	0.644478	0.62366
13.64642	0.687092	0.673769	0.660445	0.639128	0.620476
15.64052	0.691853	0.676507	0.66116	0.636605	0.615119
18.83188	0.727606	0.702402	0.677197	0.636869	0.601583

The formula shows the relationship of stress in vertical and horizontal directions:

$$\sigma_z = [(-0.0008x^2 + 0.0214x - 0.1697)\frac{C}{D} + 0.0029x^2 - 0.0795x + 1.2719]\sigma_y. \quad (10)$$

Table 6

Values σ_y in FEM

z, m	σ_y kN/m^2				
	***C/D*=1.5**	***C/D*=2**	***C/D*=2.5**	***C/D*=3.3**	***C/D*=4**
8.38406	14.70697	45.48453	51.75698	33.42773	30.72395
9.97974	70.99307	34.55252	31.36562	66.1367	69.47639
11.38978	60.24304	92.43649	99.00351	98.25886	117.2908
13.64642	65.28522	94.81899	120.7609	153.3606	213.5641
15.64052	153.2471	158.2327	169.1545	208.3287	296.7107
18.83188	152.6218	185.3962	218.5622	278.1142	338.1551

Based on Table 6 and combined with Equation (10), we find σ_z as Table 7.

Table 7

Stress in horizontal direction σ_z calculated by Equation (10)

z, m	σ_y kN/m^2				
	***C/D*=1.5**	***C/D*=2**	***C/D*=2.5**	***C/D*=3.3**	***C/D*=4**
8.38406	10.87496	32.57535	35.86385	21.91909	19.14578
9.97974	50.66223	24.03879	21.26	42.93361	43.36007
11.38978	42.05027	63.14709	66.16108	63.32565	73.14954
13.64642	44.85694	63.88606	79.75595	98.01708	132.5113
15.64052	106.0245	107.0455	111.8382	132.6231	182.5125
18.83188	111.0486	130.2226	148.0096	177.1224	203.4282

After having results from Equation (10), we compare the figures with the results from FEM. The comparison are shown in Fig. 18 to Fig. 22.

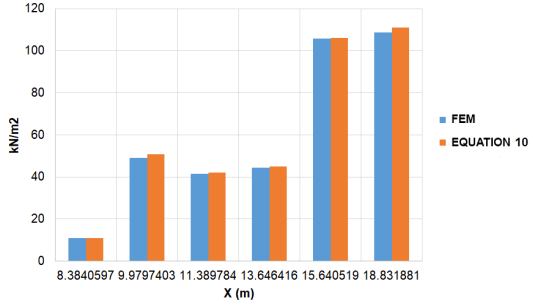

Fig. 18. Deviation σ_z by FEM and Equation (10) at *C/D*=1.5

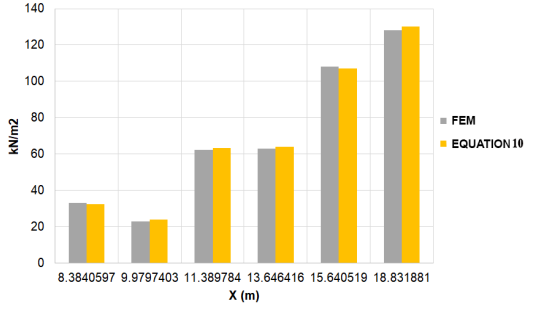

Fig. 19. Deviation σ_z by FEM and Equation (10) at *C/D*=2.0

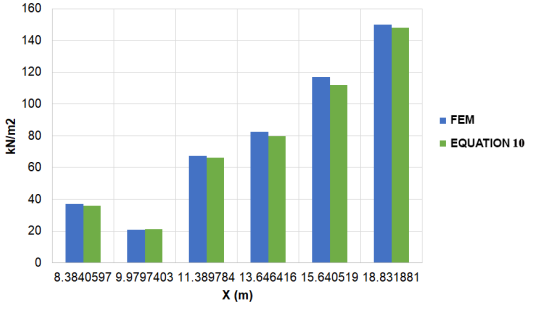

Fig. 20. Deviation σ_z by FEM and Equation (10) at *C/D*=2.5

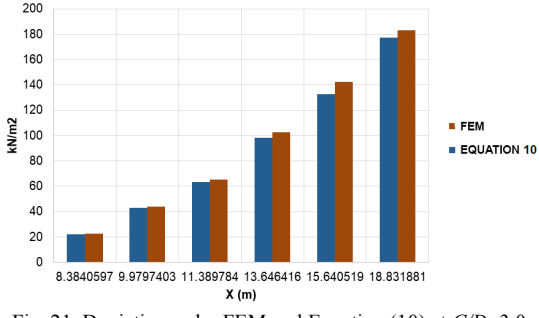

Fig. 21. Deviation σ_z by FEM and Equation (10) at *C/D*=3.0

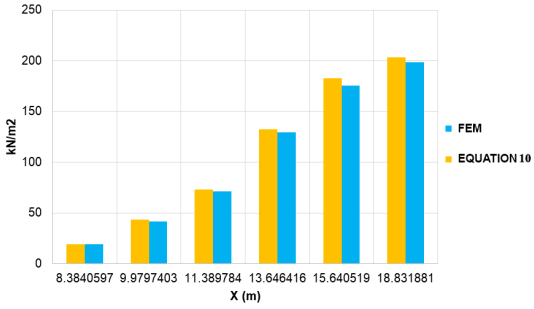

Fig. 22. Deviation σ_z by FEM and Equation (10) at C/D=4.0

It can be seen that the calculated results of stress in vertical and horizontal direction in front of tunnel face from Formula (10) and results from FEM are approximately the same. Thus, under similar geological conditions, we can use the proposed formula by the author to calculate the passive failure pressures in front of the tunnel face.

3. Conclusion

From the results of the calculation, the following conclusions can be drawn:

- It is important to determine the tunnel pressure during the construction process, the greater the depth of tunnel is, the greater the stress in front of tunnel face is. Therefore, it is necessary to calculate the minimum amount of bentonite to avoid the instability of tunnel face.

- For the small errors, it can refer to the given formula to determine the stress in front of tunnel face in the vertical and horizontal directions. However, it is also necessary to refer to results from other methods to obtain the most accurate data because this study only consider a certain geological form, which can result in some mistakes. In addition, the paper has not mentioned changes in groundwater level, rainfall and the existing load on the ground.

REFERENCES

1. Anagnostou, G., & Kovari, K. (1994), The face stability of slurry-shield-driven tunnels.Tunnelling and Underground Space Technology incorporating Trenchless, 9(2), 165-174.
2. Anagnostou, G., & Kovari, K. (1996), Face Stability Conditions with Earth-PressureBalanced Shields. Tunnelling and Underground Space Technology, 11(2), 165-173.
3. Atkinson, J. H., Brown, E. T. and Potts, D. M. (1975), Collapse of shallow unlined tunnels in dense sand. Tunnels and Tunnelling, Vol. 3, pp. 81-87.
4. Broms, B. B. and Bennermark, H. (1967), Stability of clay at vertical openings. ASCE Journal of Soil Mechanics and Foundation Engineering Division SM1, Vol. 93, pp. 71-94.
5. Brinkgreve R. B. J. and Vermeer P. A. (2001), PLAXIS Finite Element Code for Soil and Rock Analyses. A. A. Balkema, Rotterdam.
6. Chambon, P., Corte, J. F. (1994), Shallow tunnels in cohesionless soil: stability of tunnel face. Journal of Geotechnical Engineering - ASCE, 120(7), pp.1148-1165.
7. Davis, E. H., Gunn, M. J., Mair, R. J., Seneviratne, H. N. (1980), The stability of shallow tunnels and underground openings in cohesive material. Geotechnique, 30(4), pp. 397- 416.

8. Dias, D., Janin, J. P., Soubra, A. H., & Kastner, R. (2008), Three-dimensional face stability analysis of circular tunnels by numerical simulations. In Geotechnical Special Publication, (eds), pp. 886-893.
9. Kanayasu S, Kubota I, Shikibu N (1995), Stability of face during shield tunneling-A survey of Japanese shield tunneling. In: Fujita K, Kusakabe O (eds) Proceedings Underground Construction in Soft Ground. New Delhi, pp 337-343.
10. Leca, E., & Dormieux, L. (1990), Upper and lower bound solutions for the face stability of shallow circular tunnels in frictional material. Geotechnique, 40(4), 581-606.
11. Luca Borio (2008), Characterization of soil conditioning for mechanized tunnelling. UNITRACC.
12. Mair, R. J., Gunn, M. J. and O'Reilly, M. P. (1981), Centrifugal testing of model tunnels in soft clay. Presented at the 10th International Conference on Soil Mechanics and Foundation Engineering, Vol.1, pp. 323-328.
13. Mollon, G., Dias, D., Soubra, A. H., (2010), Face Stability Analysis of Circular Tunnels Driven by a Pressurized Shield. Journal of Geotechnical and GeoEnvironmental Engineering, 136(1), 215-229.
14. O'Reilly, M. P. and New, B. M. (1982), Settlements above tunnels in the United Kingdom - their magnitude and prediction. Tunnelling '82, Papers Presented at the 3 International Symposium, Institute of Mining and Metallurgy, London, England, pp. 173-181.
15. 15. O'Reilly, M. and New, B. (1998), Evaluating and predicting ground settlements caused by tunneling in London clay. Proceedings of Tunneling Symposium.
16. Oblozinsky, P., & Kuwano, J. (2004), Centrifuge experiments on stability of tunnel face. Slovak Journal of Civil Engineering (3), 23-29.
17. Sagaseta. C. (1987), Analysis of undrained soil deformation due to ground loss. Géotechnique, Vol.37, No.3, pp. 301-320.
18. Sang-Hwan Kim (1996), Model testing and analysis of interactions between tunnels in clay. DPhil Thesis, Oxford University.
19. Sang-Hwan Kim (1996), Evaluation of Shield Tunnel Face Stability in Soft Ground. International Symposium on Underground Excavation and Tunnelling, pp 213-220.
20. Shirlaw, J. N., (1995), Observed and calculated pore pressures and deformation induced by an earth balace shield: Discussion. Canada Geotech, J. 32, pp. 181-189.
21. Soubra, A. H. (2002), Kinematical approach to the face stability analysis of shallow circular tunnels. Proceedings of the Eight International Symposium on Plasticity, 443-445.
22. Soubra, A. H., Dias, D., Emeriault, F., & Kastner, R. (2008), Three-dimensional face stability analysis of circular tunnels by a kinematical approach. Geotechnical Special Publication, 894-901.
23. Talebinejad, A. et al (2011), Numerical and empirical analysis of face pressure effect on surface subsidence at a tunnel excavated by EPB method. First Asian and 9th Iranian Tunnelling Symposium.
24. Vardoulakis, P., Maria Stavropoulou, George Exadaktylos (2009), Sandbox modeling of the shallow tunnel face collapse. Rivista Italiana Di Geotenica 1/2009, pp. 9-22.
25. Vermeer, P. A., Nico Ruse and Thomas Marcher (2002), Tunnel Heading Stability in Drained Ground. FELSBAU 20, pp. 8-18.
26. Verruijt, A. and Booker, J. R. (1996), Surface settlements due to deformation of a tunnel in an elastic half plane. Géotechnique, Vol. 46, No. 4, pp. 753-756.
27. WONG Kwong Soon (2012), Passive failure and deformation mechanisms due to tunnelling in sand and clay. PhD. Thesis, The Hong Kong University of Science and Technology.

Стаття надійшла до редакції 03.05.2020

Nguyen Anh Tuan, Tran Van Dung

ESTABLISHING THE CORRELATION OF THE VERTICAL AND HORIZONTAL PASSIVE FAILURE PRESSURE IN FRONT OF CONSTRUCTED TBM TUNNELS FACE IN SAND

The paper aims to investigate the relationship between factors which have the impacts on the tunnel and the ground and establish formulas to calculate the correlation of the passive failure pressure in front of tunnel face in the vertical and horizontal directions by using the Finite Element Method (FEM).

Keywords: TBM tunnel, FEM, passive failure pressure, tunnel face, sand.

Нгуен Ань Туан, Чан Ван Зунг

ВИЗНАЧЕННЯ СПІВВІДНОШЕННЯ ВЕРТИКАЛЬНОГО І ГОРИЗОНТАЛЬНОГО ПАСИВНИХ ТИСКІВ ДЕФОРМОВАНОСТІ ГРУНТІВ ПРИ СПОРУДЖЕННІ ТБМ ТУНЕЛЮ

Метою статті є дослідження взаємозв'язку факторів, що впливають на тунель та основу, та визначити формули для розрахунку кореляції тиску пасивного руйнування перед торцем тунелю у вертикальному та горизонтальному напрямках за допомогою методу кінцевих елементів (МСЕ).

Ключові слова: ТБМ тунель, МСЕ, пасивний тиск руйнування, грань тунелю, пісок.

UDC 539.3
Nguyen Anh Tuan, Tran Van Dung. **Establishing the correlation of the vertical and horizontal passive failure pressure in front of constructed tbm tunnels face in sand** // Strength of Materials and Theory of Structures: Scientific-and-technical collected articles. – K.: KNUBA, 2020. – Issue 105. – P. 33-47.
Fig. 22. Ref. 27.

УДК 539.3
Нгуен Ань Туан, Чан Ван Зунг. **Визначення співвідношення вертикального і горизонтального пасивних тисків деформованості грунтів при спорудженні ТБМ тунелю**// Опір матеріалів і теорія споруд: наук.-тех. збірн. – К.: КНУБА, 2020. – Вип. 105. – С. 33-47.
Іл. 22. Библіогр. 27 назв.

Автор (вчена ступень, вчене звання, посада)*: PhD, Lecturer, Faculty of Transportation Engineering, Hochiminh City University of Transport, Nguyen Anh Tuan*
Адреса: *No. 2, D3 St., Ward 25, Binh Thanh Dist., Hochiminh City, Vietnam.*
Тел.: *(+84) 917.863.898.*
E-mail: *tuankct@hcmutrans.edu.vn*

Автор (вчена ступень, вчене звання, посада)*: MEng, Faculty of Transportation Engineering, Hochiminh City University of Transport, Tran Van Dung*
Адреса: *No. 2, D3 St., Ward 25, Binh Thanh Dist., Hochiminh City, Vietnam.*
Тел.: *(+84) 917.863.898.*
E-mail: *tuankct@hcmutrans.edu.vn*